

## SEQUENCE STRATIGRAPHY AND PALEONTOLOGY OF THE UPPER MIOCENE PISCO FORMATION ALONG THE WESTERN SIDE OF THE LOWER ICA VALLEY (ICA DESERT, PERU)

CLAUDIO DI CELMA<sup>1\*</sup>, ELISA MALINVERNO<sup>2</sup>, GIULIA BOSIO<sup>2</sup>, ALBERTO COLLARETA<sup>3,4</sup>, KAREN GARIBOLDI<sup>3,4</sup>, ANNA GIONCADA<sup>3</sup>, GIANCARLO MOLLI<sup>3</sup>, DANIELA BASSO<sup>2</sup>, RAFAEL M. VARAS-MALCA<sup>5</sup>, PIETRO PAOLO PIERANTONI<sup>1</sup>, IGOR M. VILLA<sup>2</sup>, OLIVIER LAMBERT<sup>6</sup>, WALTER LANDINI<sup>3</sup>, GIOVANNI SARTI<sup>3</sup>, GINO CANTALAMESSA<sup>1</sup>, MARIO URBINA<sup>5</sup> & GIOVANNI BIANUCCI<sup>3</sup>

<sup>1\*</sup>Corresponding author. Scuola di Scienze e Tecnologie, Università di Camerino, Camerino, Italy. Email: claudio.dicelma@unicam.it

<sup>2</sup>Dipartimento di Scienze dell'Ambiente e della Terra, Università di Milano-Bicocca, Milano, Italy

<sup>3</sup>Dipartimento di Scienze della Terra, Università di Pisa, Pisa, Italy.

<sup>4</sup>Dottorato Regionale in Scienze della Terra Pegaso, Pisa, Italy.

<sup>5</sup>Departamento de Paleontología de Vertebrados, Museo de Historia Natural, Universidad Nacional Mayor de San Marcos, Lima, Peru.

<sup>6</sup>D.O. Terre et Histoire de la Vie, Institut Royal des Sciences Naturelles de Belgique, Brussels, Belgium.

To cite this article: Di Celma C., Malinverno E., Bosio G., Collareta A., Gariboldi K., Gioncada A., Molli G., Basso D., Varas-Malca R.M., Pierantoni P.P., Villa I.M., Lambert O., Landini W., Sarti G., Cantalamessa G., Urbina M. & Bianucci G. (2017) - Sequence stratigraphy and paleontology of the Upper Miocene Pisco Formation along the western side of the lower Ica Valley (Ica Desert, Peru). *Riv. It. Paleontol. Strat.*, 123(2): 255-273.

**Keywords:** Pisco Formation; late Miocene; sequence stratigraphy; vertebrate and macro-invertebrate paleontology; diatom biostratigraphy; tephrochronology.

**Abstract.** The sequence stratigraphic framework and a summary of the fossil fauna of the Upper Miocene portion of the Pisco Formation exposed along the western side of the Ica River (southern Peru) is presented through a new geological map encompassing an area of about 200 km<sup>2</sup> and detailed chronostratigraphic analyses. Extensive field mapping and sedimentological study of outcrop sections have shown that the Pisco Formation is a cyclical sediment unit composed of at least three fining-upward, unconformity-bounded depositional sequences, designated P0, P1, and P2 from oldest to youngest. In the study area, these sequences progressively overlap a composite basal unconformity from southwest to northeast.

Integration of biostratigraphic and tephrochronologic age determinations constrains the ages of the three Pisco sequences within the study area. Based on the age of surrounding sediments, a conservative estimate of the age of P0 suggests deposition of these strata between 17.99 ± 0.10 Ma and 9.00 ± 0.02 Ma, whereas diatom biostratigraphy and calculated <sup>40</sup>Ar/<sup>39</sup>Ar ages converge to indicate that strata of the P1 sequence were deposited sometime between 9.5 Ma and 8.9 Ma and that those of the P2 sequence are younger than 8.5 Ma and older than 6.71 ± 0.02 Ma. Our survey for both vertebrate and macro-invertebrate remains in the three sequences confirms the outstanding paleontological value of the Pisco Formation and contributes to depict regional faunal shifts in the fossil assemblage.

## INTRODUCTION

Over the past decades, the extensive paleontological investigations that have been conducted on the Upper Miocene to Pliocene Pisco Formation exposed in the Ica Desert, southern Peru, have yielded substantial assemblages of exquisitely preserved fossil marine vertebrates, including cetaceans, pinnipeds, crocodiles, seabirds, sharks, and bony fish (e.g., Bianucci et al. 2016a, 2016b, 2016c; Stucchi et al. 2016; Landini

et al. 2017), and mollusks (DeVries 2007). The accurate placement of these discoveries into a proper stratigraphic context, however, remains a largely unresolved issue that bears upon the general lack of robust biostratigraphic and tephrochronologic age constraints and uncertain intraformational correlations (Brand et al. 2011). As a result, the paleontological research has mostly focused on systematic studies of single skeletons, the ecology of fossil vertebrates, and the processes governing their preservation, abundance, and taphonomy (Muizon 1988; Brand et al. 2004; Esperante et al. 2008, 2015; Lambert et al. 2009, 2010a, 2010b, 2014, 2015, 2017a, 2017b; Bianucci et

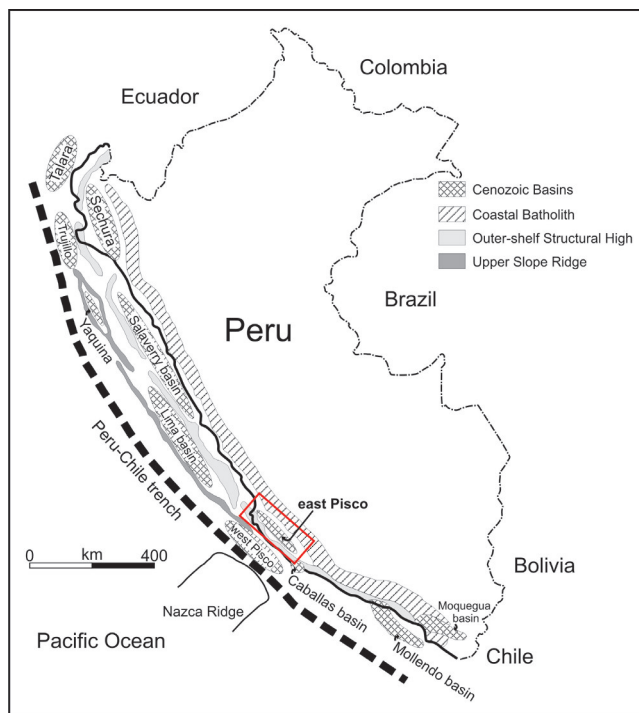


Fig. 1 - Sketch map of the major sedimentary basins of coastal Peru showing position of both the Outer Shelf Ridge and Upper Slope Ridge, redrawn and modified from Travis, Gonzales, & Pardo (1976) and Thornburg & Kulm (1981).

al. 2010, 2016a; Collareta et al. 2015, 2017; Gariboldi et al. 2015; Gioncada et al. 2016). By contrast, correlations of individual fossil findings to temporally constrained measured sections have only been established for two important fossil-bearing localities (Bianucci et al. 2016b, 2016c), where comprehensive stratigraphic frameworks were recently established (Di Celma et al. 2016a, 2016b).

The primary objectives of this paper, which is focused on the portion of the Pisco Formation exposed south of the Ocucaje village, along the western side of the Ica River, are: i) to set the stratigraphic cyclicity evident in the architecture of the Pisco Formation within a sequence stratigraphic framework; ii) to constrain the age of the three unconformity-bounded depositional sequences through the integration of radiometric dating of volcanic ash layers and diatom biostratigraphy; and iii) to provide a summary of the vertebrate and macro-invertebrate fossil assemblages found within these Upper Miocene marine strata. These developments represent a first step in facilitating correlation between scattered and geographically disparate outcrop sections and provide a sound basis for future studies on the systematics, comparative morphology, phylogeny and paleoecology of Pisco fossil verte-

brates and the biological and physical factors dictating their distribution and evolutionary trends.

## REGIONAL TECTONICS AND STRATIGRAPHIC BACKGROUND

**Geological setting.** The regional tectonic setting of the Peruvian margin is dominated by the oblique subduction of the Nazca/Farallon Plate underneath the South American Plate in the Peru-Chile Trench. This subduction, which began in the Cretaceous and continues today, developed a composite transform-convergent margin characterized by normal and strike-slip faults (e.g., Barazangi & Isacks 1979; Pilger 1981; Cahill & Isacks 1992; León et al. 2008; Zúñiga-Rivero et al. 2010).

According to Thornburg & Kulm (1981), two long and narrow structural ridges, the Outer Shelf Ridge and the Upper Slope Ridge, were formed on the continental shelf and upper slope of the Peruvian continental margin by late Cretaceous – early Paleogene tectonic activities that involved Paleozoic and Mesozoic strata. These two ridges and associated shorter, transverse shelf uplifts, or local highs, subdivided the Peruvian offshore into a series of Cenozoic sedimentary basins (Fig. 1). In coastal southwestern Peru, the most westerly Upper Slope Ridge separates the Pisco basin into an offshore and an onshore portion, referred to as the West Pisco basin and East Pisco basin, respectively. Rapid uplift and emersion of the Cenozoic fill and underlying composite basement of the East Pisco basin is interpreted to be related to subduction of the aseismic Nazca Ridge beneath this part of Peruvian forearc during the Quaternary (e.g., Hsu 1992; Macharé & Ortlieb 1992; von Huene et al. 1996; Hampel et al. 2002).

**Stratigraphic overview.** The sedimentary fill of the East Pisco basin has been described by Dunbar et al. (1990) and DeVries (1998) and consists of four lithostratigraphic units: the middle to upper Eocene Paracas Formation, the uppermost Eocene-lower Oligocene Otuma Formation, the uppermost Oligocene to lower Miocene Chilcatay Formation, and the Upper Miocene to Pliocene Pisco Formation. These units are underlain by a deformed and heterogeneous basement including lower Paleozoic intrusive rocks and Jurassic volcano-sedimentary rocks. The above mentioned Cenozoic formations are bounded by

regionally extensive, conglomerate-mantled unconformities that are locally accompanied by angular discordances and document relatively long breaks in sedimentation.

## STUDY AREA AND METHODS

The detailed stratigraphic and mapping work of the Pisco Formation provides the necessary context for the sequence stratigraphy, chronostratigraphy, and paleontology presented in this study. It was conducted over the course of three field campaigns between 2015 and 2016 and encompasses an area of approximately 200 km<sup>2</sup> that stretches for 22 km along the western side of the Ica River valley, from Cerro Blanco in the north to Cerro las Tres Piramides in the south (Fig. 2 in Appendix 2). In order to accurately reconstruct the stratigraphy of the strata exposed in this area, the field portion of the investigation included: i) geological mapping at 1:10,000 scale; ii) structural analysis of faults identified through interpretation of high-resolution Google Earth imagery; iii) measuring of four detailed outcrop sections; and iv) collection of rock samples for micropaleontological analyses, <sup>40</sup>Ar/<sup>39</sup>Ar age determination, and geochemical and mineralogical characterization of volcanic ash layers.

The fossil content of the three Pisco sequences was assessed by prospecting for fossil remains in the mapped area and integrated with data from the well-investigated sites of Cerro Colorado (Bianucci et al. 2016c) and Cerro los Quesos (Bianucci et al. 2016b).

Radiometric dating has been carried out on selected volcanic ash layers that have been chosen based on lack of post-depositional reworking structures and alteration marks, their strategic position in the stratigraphic succession, and the presence of biotite crystals, which have shown to give better results than feldspars (Gariboldi et al. 2017). Ash layers have also been selected according to the results of microprobe analyses, which have been performed by using a JEOL 8200 Super Probe at the University of Milan: the suitable ash layers have a single and homogeneous population of biotite crystals that does not show any loss of K in the interlayer occupancy. <sup>40</sup>Ar/<sup>39</sup>Ar age estimations have been done by the step-heating method (Villa et al. 2000) with NuInstruments™ Noblesse® noble gas mass spectrometer at the University of Milano-Bicocca.

## RESULTS

**Cenozoic stratigraphy.** The Cenozoic stratigraphic record exposed across the study area comprises two distinct formations, namely the Chilcatay and Pisco formations. Close to the basin margins, these two units rest nonconformably onto a paleosurface carved into a complex basin basement including lower Paleozoic gabbroic to granitoid rocks of the San Nicolás batholith and Jurassic volcano-sedimentary rocks of the Guaneros Formation (Mukasa & Henry 1990; León et al. 2008).

### *Chilcatay Formation.*

The lower portion of the Chilcatay Formation comprises brownish to light coloured, fine- to very coarse-grained biocalcarenite variably mixed with siliciclastic sediment and gently dipping to the southeast. These sediments underlie and, locally, landward interfinger (from southwest to northeast) with a seaward-dipping, 20 m-thick clinofomed wedge within which reworked pectinids, oysters and barnacle plates account for a large portion of the highly degraded skeletal fraction. At Cerro las Tres Piramides, a spectacular section in these biocalcarenitic sediments of the Chilcatay Formation displays well-developed clinofom geometry with planar to tangential foreset beds steeply dipping to the southwest. Similar cool-water carbonate wedges with seaward dipping, steep clinofoms and significant along-strike extension have been documented by Pomar & Tropeano (2001) and Massari & Chiocci (2006) on relatively steep margins characterized by tectonically structured and physiographically complex shelves.

The clinostratified calcarenitic wedge is unconformably overlain by a northeast dipping, fining upward unit composed of basal sandstones passing upward into interbedded siltstones, dolomitized mudstone horizons and volcanic ash layers (DeVries & Schrader 1997). This stratal wedge, which is characterized by a lack of preserved vertebrate fossils, is about 10 m thick at Cerro las Tres Piramides and about 25 m thick at Cerro Yesera de Amara.

### *Pisco Formation.*

Within the study area, the little deformed and richly fossiliferous Pisco Formation forms a northeastward dipping monocline possibly developed in response to subduction of the Nazca Ridge beneath

the region during the Quaternary (Hampel 2002). Integration of several partial stratigraphic sections indicates that the composite thickness of the Pisco Formation in the study area is about 470 m. Owing to lateral thickness and facies variations and the limited capacity of lithostratigraphic mapping to reveal the genetic and depositional history of the Pisco Formation, field mapping has been carried out through the construction of a detailed sequence stratigraphic framework. Based on the occurrence of three widespread erosional surfaces, designated PE0.0, PE0.1, and PE0.2 from oldest to youngest, the strata can be subdivided into three genetic packages (depositional sequences) that have been named P0, P1, and P2 for their lower bounding surface. These three unconformities converge and merge landwards into a single surface (informally referred to as PE0) representing the composite lower boundary of the Pisco Formation. Strata between successive unconformities exhibit a deepening-upward, transgressive trend, in which downdip facies associations step up over updip facies associations. Regressive facies successions are lacking, either because regression was non-depositional or because regressive deposits were eroded during the phase of subaerial exposure and/or during next transgression.

Sequence bounding unconformities are of basinal extent and indicate abrupt seaward shifts in facies (Fig. 3a). These surfaces are commonly demarcated by a *Glossifungites* ichnofacies (Fig. 3b, c) dominated by *Thalassinoides* and flask-shaped *Gastrochaenolites* that are excavated into a semiconsolidated (firm-ground) substrate and reflect a break in sedimentation, generally accompanied by erosion (e.g., Pemberton et al. 1995). The *Glossifungites*-demarcated erosional discontinuities are mantled by coarse-grained, relatively thin (up to 0.4 m thick) intervals including a variable mixture of pebble- to boulder-size lithic clasts, pebble-sized phosphatic nodules, cobble-sized dolomite clasts showing bivalve borings, internal molds of gastropods and articulated bivalves, shark teeth, polished bone fragments, and partially articulated skeletons of marine mammals (Fig. 3). This coarse-grained facies rests below deposits indicative of marine flooding and above a surface indicating abrupt seaward shift in facies and, therefore, it is regarded as a transgressive lag representing erosion and low net sedimentation rates during shoreface retreat (e.g., Grimm 2000;

Boessenecker et al. 2014; Föllmi 2016). A subaerial origin for the basal unconformities is also corroborated by the presence of basement clasts, which were probably introduced into the basin during periods of lowered sea level and reworked by waves and currents during subsequent marine transgression.

The transgressive lag is directly overlain by a sand-rich units comprising yellow-weathering, fine- to very fine-grained sandstones and coarse siltstones that are typically moderately to highly bioturbated and, locally, showing unidirectional cross-bedding, swaley cross-stratification, and wave ripples. Vertebrate material is locally abundant and includes disarticulated to partially articulated marine mammal skeletons. The array of primary sedimentary structures represents unidirectional- or combined-flow erosion and waning oscillatory flow and indicates lower shoreface deposition above fair-weather wave base.

The diatomaceous mudstones consist of finely laminated gray-white diatomite, rich in planktonic diatoms characteristic of a highly productive marine environment. Subordinate lithologies include volcanic ash layers, dolomitized mudstone horizons, and thin, fine- to medium-grained sandstone beds. These sediments are sparsely fossiliferous and vertebrate fossils vary in preservation from disarticulated to fully articulated skeletons. Macro-invertebrate body fossils are rare and usually limited to internal molds lacking calcium carbonate skeletal material. The diatomaceous mudstones are reflective of deposition from suspension of organic-rich mud in a low-energy offshore shelf environment. Facies composition of a single depositional sequence changes predictably up depositional dip, so that when traced towards the northeast, the offshore diatomaceous mudstones grade laterally into a sandstone-dominated succession comprising abundant swaley cross-stratification and unidirectional cross-bedding with occasional phosphate pebble beds overlying sharp, gutter-casted erosion surfaces. This assemblage of sedimentary structures is indicative of deposition in a shoreface setting strongly influenced by storms (e.g., Leckie & Walker 1982; Chiocci & Clifton 1991; Myrow 1992). As a consequence, the bounding unconformities that in more distal areas are demarcated by abrupt basinward shift of facies, become subtle sand-on-sand contacts in more proximal areas.

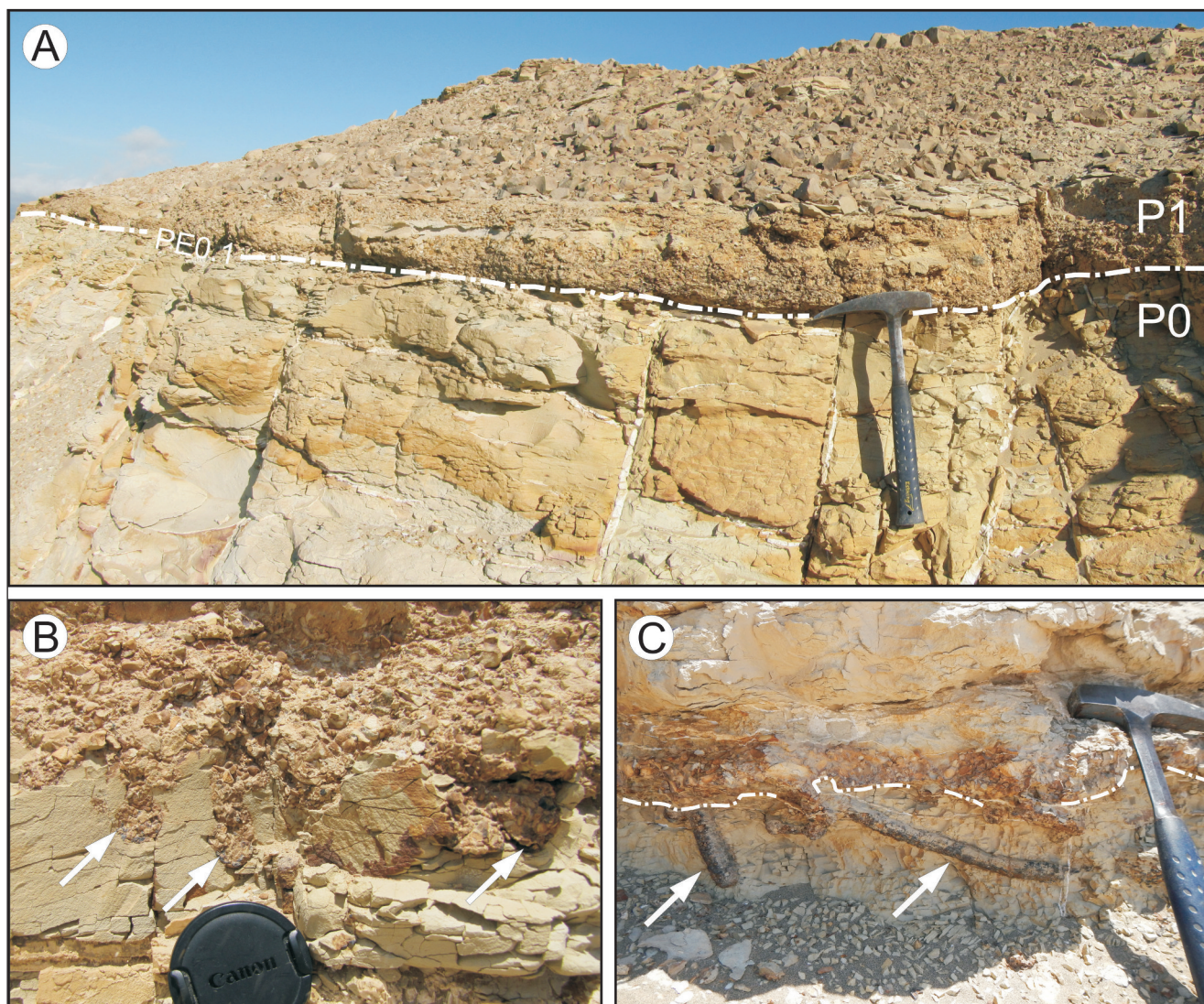


Fig. 3 - Details of the intraformational unconformities. A lens cap (6.5 cm in diameter) and a hammer (0.3 m long) are used for scale. A) Outcrop photograph of PE0.1 at Cerro las Tres Piramides ( $14^{\circ}35'15''\text{S}$  -  $75^{\circ}38'38''\text{W}$ ). This surface is overlain by a lag comprised of rounded phosphate and igneous pebbles, reworked shells, and bones. B) The surface itself is generally sharp and undulating, bored and penetrated by robust *Thalassinoides* burrows (arrowed), which pipe dark phosphate pebbles of the P1 sequence for 0.3 m into the underlying P0 sequence. C) Detail of PE0.0 ( $14^{\circ}35'41''\text{S}$  -  $75^{\circ}40'5''\text{W}$ ) showing inclined, smooth-walled *Thalassinoides* shafts weathering out in positive relief (arrowed) and passively filled with granular phosphorite infiltrated from the overlying pebble lag.

*P0* sequence. Sediments of the P0 sequence are best exposed in the southeastern corner of the mapped area, where they crop out in the lower half of a series of small, isolated *cerros* or hills (namely, Cerro Yesera de Amara, Cerro Submarino, Cerro Buque, Cerro las Tres Piramides, Cerros los Tinajones) and rest with angular unconformity on variably deformed rocks of the Chilcatay Formation (Fig. 4a). At Mal Paso, immediately to the southeast of Cerro Yesera de Amara, the PE0.0 basal unconformity is characterized by truncation of the underlying strata and is marked by a prominent marine transgressive surface indicated as the M1 marker bed by Brand et al. (2011). In this area, however, our correlation

of the P0 outcrop belt differs somewhat from that proposed by Brand et al. (2011). At Cerro Submarino and Cerro Buque these authors correlated our PE0.0 surface to their similar, but stratigraphically higher, M2 stratigraphic marker. We argue that the interpretation proposed by Brand et al. (2011) should be revised and that at these two localities the M2 marker defined by Brand et al. (2011) at the base of the hills is, in fact, their M1 marker (PE0.0 surface in our terminology).

This unit is strongly wedge-shaped, thinning from 40 m in the southeastern portion of the study area (Cerro las Tres Piramides, Fig. 4a), to a zero-edge in the vicinity of Cerro la Bruja over approximately 6

km. Rather than elimination at the top by erosion, it seems more likely that the primary reason for gross stratal thinning is progressive onlap and loss of successively younger beds at the base. Between Cerro las Tres Piramides and Cerro la Bruja this unit also shows pronounced lateral facies changes with offshore mudstones dominating the unit in the south rapidly replaced northwards by fine- to very coarse-grained, cross-stratified, fossil-rich nearshore calcarenites.

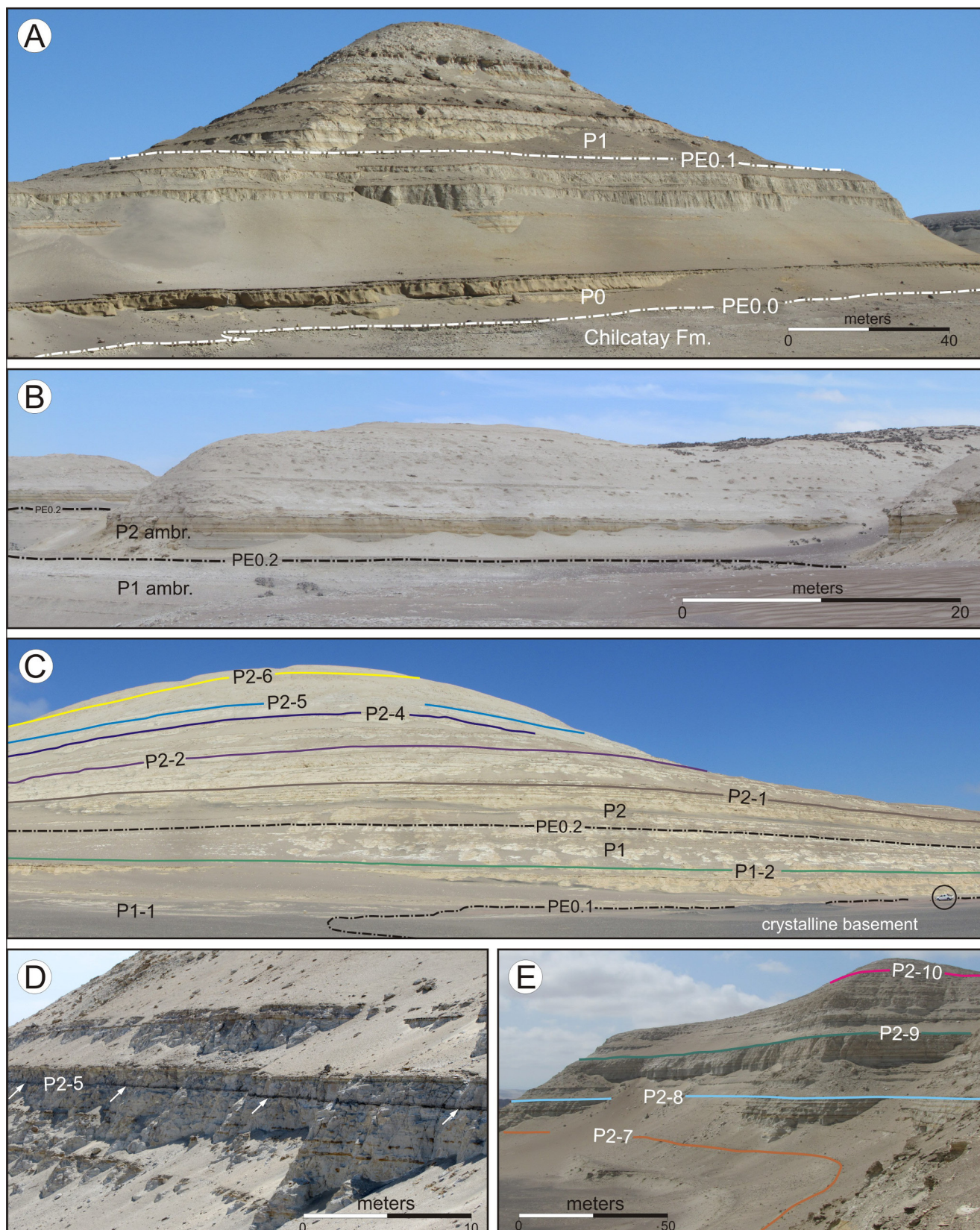
The vertebrate content of this unit is less well known than that from P1 and P2 and most of the observations come from the on-going study of three localities (Mal Paso, Yesera de Amara and north of Cerro Submarino). Mysticetes (baleen-bearing whales) are common and represented by at least three species: a large-sized stem balaenopteroid (Balaenopteroidea, rorquals and relatives) similar to *Pelocetus*, a smaller *Parietobalaena*-like form, and a rare cetotheriid (Cetotheriidae) that shares some similarities with the species recognized in P1 (see below). Odontocetes (toothed whales) consist of a few specimens belonging to at least one physeteroid species and two kentriodontid-like delphinidan species. A single indeterminate pelagornithid skeleton is the only bird specimen found up to now. Fragmentary remains attributed to chelonoid sea turtles and long-snouted crocodylians are also recorded. Shark tooth-rich horizons have not been recognized to date, nevertheless, teeth attributed to the giant mega-toothed shark *Carcharocles megalodon* and to *Cosmopolitodus hastalis* occur in this unit along with abundant remains of Myliobatiformes (including the eagle ray *Myliobatis*). Moreover, teeth belonging to the extinct snaggletooth shark *Hemipristis serra* are relatively common in P0; this fossil shark species is present in the underlying deposits of the Chilcatay Formation, whereas it is absent from the younger P1 and P2 sequences. Several associated rostral spines of a pristid sawfish were also collected from strata belonging to the P0 sequence.

With regard to invertebrates, in the north of Cerro Yesera de Amara, Cerro Submarino and Cerro Sombrero, where P0 crops out, some internal molds of the bivalve genus *Chionopsis* have been found just above the base and in the upper part of this sequence. North of Cerro Submarino some specimens of large *Dosinia ponderosa*, along with *Miltha* sp. and specimens of Ostreidae have been recognized a few meters above the PE0.0 surface, showing a

calcite composition of shells. Concerning gastropods, some specimens belong to the family Architectonicidae and an exemplar of Cypraeidae have been found; only two other specimens of this family, as the holotype of *Muracypraea ormenoii*, has ever been documented in the Pisco Basin by DeVries et al. (2006). In the same locality, some barnacle plates have been found, preserving the calcite composition. Finally, *Turritella infracarinata*, *Tactilispina vermeiji*, *Amiantis* sp. and *Ficus distans* have also been recognized in P0 (DeVries pers. com.).

*P1 sequence.* This depositional sequence is bounded by PE0.1 at the base and PE0.2 at the top (Fig. 4a, b). The PE0.1 basal surface has been indicated as the M2 marker by Brand et al. (2011) and can be

Fig. 4 - Outcrop photos showing some of the marker beds and the three key surfaces that have been mapped in the study area. The three erosive surfaces, referred to as PE0.0, PE0.1, and PE0.2 in ascending order, are readily recognizable in the field based on a seaward shift in facies from outer shelf diatomaceous mudstones to nearshore sandstones. A) Panoramic view of the Cerro las Tres Piramides section (14°35'30"S - 75°38'45"W), near the southeastern end of the study area, showing two Pisco depositional sequences (namely P0 and P1) and their two bounding surfaces (PE0.0 and PE0.1). View is to the south. Note that the basal sand-rich units of the two sequences pass conformably up-section into finer-grained diatomaceous siltstones marking deepening from the underlying nearshore facies into offshore facies. B) View of the contact between the P1 and P2 sequences at Cerros Cadenas de los Zanjones (14°34'55"S - 75°42'56"W). Diatomaceous mudstones form gentle slopes whereas thick resistant sandstones at the base of the P2 sequence form a wide ledge and a vertical cliff between the slopes. C) Panoramic view of the eastern side of Cerro la Bruja (14°31'55"S - 75°39'46"W); circled car for scale. Here, the P1-1 marker bed is on the valley floor and onlaps the crystalline basement, whereas the P1-2 forms a prominent ledge at the base of the cliff. The PE0.2 bounding surface is at the base of the yellowish, cliff-forming basal sandstone unit correlative of "La Bruja vertebrate level". The P2-1 marker bed is the uppermost of a set of visually distinct brown very fine-grained sandstones alternating with softer siltstones (M3 marker bed of Brand et al. 2011). The P2-2 marker bed forms a wide terrace-like ledge at the northern end of Cerro la Bruja (14°31'17"S - 75°39'50"W). At this site, P0 is not present, having lapped out northwards onto surface PE0.0. Traced northeastward, P2 oversteps P1 strata thinning and onlapping onto crystalline basement. D) Close view of the western side of Cerro la Bruja (14°31'39"S - 75°40'1"W) showing the P2-5 marker bed (arrowed), a characteristic blackish vitric tuff with soft-sediment deformed laminae. E) Panoramic view showing some of the marker beds traced along the cliff-slope profile of the eastern side of Cerro Hueco la Zorra (14°26'40"S - 75°41'20"W). The P2-8 marker bed (M 10 of Brand et al. 2011) is about 0.5 m thick and includes a phosphate pebble bed overlain by a relatively resistant, ledge-forming, thinly-bedded sandstone. Both P2-9 and P2-10 are prominent and laterally continuous ledges at the top of sheer cliff faces.



traced from the south (Cerro Yesera de Amara, Cerro Submarino, Cerro Buque, Cerro las Tres Piramides, Cerro los Tinajones, Cerros la Mama y la Hija) to the central part of the study area, near the

southern end of the lower slopes of Cerro el Brujito. The P1 sequence attains a maximum thickness of about 80 m in the southwest (Cerros Cadenas de los Zanjones) and thins towards northeast to about

40 m at Cerro la Bruja, beyond which it is supposed to pinch out by progressive onlap onto basement rocks.

The vertebrate content of this highly fossiliferous unit is known from various localities of the Ica Desert, including Cerro Colorado outside of the study area (“lower allomember” of Di Celma et al. 2016b; Bianucci et al. 2016c) and Cerro la Bruja and Cerros Cadenas de los Zanjones within it. A significant fraction of the vertebrates detected in this unit are found enclosed in more or less developed dolomite concretions (Gariboldi et al. 2015). Mysticetes are abundant and consist of several skeletons belonging to an undescribed large-sized cetotheriid species, and of a few other remains belonging to two indeterminate balaenopterid species (Collareta et al. 2015; Gioncada et al. 2016). Among the odontocetes, the stem physeteroids include the holotype and only known specimen of the giant raptorial sperm whale *Livyatan melvillei* and several *Acrophyseter*-like specimens (Lambert et al. 2010a; Lambert et al. 2017a; pers. obs). The ziphiids (beaked whales) are represented by two stem species: the very common *Messapicetus gregarius* and *Chimuziphius coloradensis* (only known for the holotype skull) (Bianucci et al. 2010, 2016a; Lambert et al. 2010b). Delphinidans consist of two pontoporiids (the abundant *Brachydelphis mazzeasi* and a less common, undescribed species somewhat resembling *Pliopontos littoralis*), one inioid (*Brujadelphis ankylostris*) known for a single specimen described by Lambert et al. (2017a), and several specimens of kentriodontid-like delphinidans (belonging to at least two species). Birds are known from well-preserved skeletons referred to two medium- and large-sized sulids (boobies: *Sula brandi* and *S. figueroae*) and fragmentary remains referred to indeterminate phalacrocoracids (cormorants) and procellariids (Stucchi et al. 2016). The pancheloniid sea turtle *Pacificheys urbinai* is represented by various well-preserved specimens (Parham & Pyenson 2010). Indeterminate crocodylian remains have also been recognized. Shark teeth are common all along the studied section, although they particularly concentrate in two intervals. The chondrichthyan assemblage is well diversified but dominated by Carcharhiniformes (mostly represented by teeth belonging to *Carcharhinus* spp.); Lamniformes (including the large species *Carcharocles megalodon* and *Cosmopolitodus hastalis*) and Myliobatiformes are also well represented, whereas pristids and squatinids are

present but overly rare (Landini et al. 2017). Bony fish include ubiquitous cycloid scales referred to the Pacific pilchard *Sardinops* sp. cf. *S. Sagax*; sciaenids (drums), and scombrids (aff. *Thunnus* sp.) were also detected. Among the Ica Desert localities in which P1 strata are exposed, Cerro Colorado features some examples of exceptional fossil preservation, such as the stomach contents of two cetaceans (a specimen of *Messapicetus gregarius* and a medium-sized cetotheriid), revealing predation upon *Sardinops* (Collareta et al. 2015; Lambert et al. 2015), and the fossilized baleen of a balaenopteroid whale (Gioncada et al. 2016).

The P1 sequence is characterized by a relatively abundant and varied mollusk assemblage, especially at its base, where all the specimens are internal molds composed of dolomite. At the base, which crops out at Cerros Cadenas de los Zanjones, bivalves belong to the genera *Dosinia* (*D.* cf. *ponderosa*), *Hybolophus*, *Miltha* and *Trachycardium*. At Cerro Sombrero, the most common bivalves are *Chionopsis* sp.; at the same level, tonnoid gastropods also occur. A particular assemblage has been found southeast of Cerro Colorado, a locality 25 km northwest of the study area: at one level, a few meters above the base of the P1 sequence, large dolomite molds occur, as the bivalve genera *Panopea* and *Trachycardium*, along with specimens of different sizes of *Dosinia* cf. *ponderosa*, and fossil plates of barnacles. At Cerro Colorado, many dolomite molds and gypsum-replaced shells of *Anadara sechurana* and *Dosinia* sp. have been found at the same level of a kentriodontid-like delphinidan fossil, where strata of the P1 sequence crop out. At Cerro los Quesos, immediately to the west of the present study area, a level characterized by dolomitic internal molds of *Hybolophus* sp. is present. Near Cerros Cadenas de los Zanjones, the mollusk assemblage is composed of many dolomitic molds of *Dosinia* cf. *ponderosa*; *Miltha* sp. and *Hybolophus* sp.; gastropods of the superfamily Tonnoidea and the turritellid *Incatella hupei*. Finally, near Cerro La Bruja the mollusk assemblage includes *Hybolophus* sp., *Turritella varicosta*, *Trachycardium* sp., *Anadara sechurana* and *Dosinia* sp. with specimens differing from *D. ponderosa* for size, shape and ornamentation of the shell.

*P2 sequence.* The PE0.2 surface at the base of the P2 sequence is exposed from Cerros Cadenas de los Zanjones in the southwest (Fig. 4b), through Cerros la Mama y la Hija and Cerro Yesera de Amara

in the south, to Cerro Blanco in the north. At Cerro La Bruja (Fig. 4c) the overlying, richly fossiliferous interval is sometimes referred to as the “La Bruja vertebrate level” (Muizon & DeVries 1985; Muizon 1988).

Due to onlap and loss of successively younger beds at the base, P2 forms a northeastward-thinning wedge with a general dip of strata between 4° and 7° to the northeast. For mapping purposes, ten distinctive stratigraphic markers consisting of distinctively weathering units of varying lithology, informally designated P2-1 to P2-10, have been traced with reasonable confidence between Cerro la Bruja and Cerro Blanco (Fig. 4c, d, e). In this study, the P2-1, P2-7, and P2-8 marker beds correspond with M3, M9, and M10 of Brand et al. (2011), respectively. Lateral tracing of these marker beds shows that the shallow-water strata of the P2 sequence onlap an unconformity surface cut across the P1 sequence, which they overstep north of Cerro el Brujito to onlap onto basement crystalline rocks.

The PE0.2 bounding surface can be traced into outcrop belts to the west (Cerro los Quesos) and northwest (Cerro Colorado) of the present study area, where detailed stratigraphic frameworks were already established by recent studies (Di Celma et al. 2016a, 2016b). At Cerro los Quesos, the PE0.2 unconformity can be traced into a prominent lithological contact documented by Di Celma et al. (2016a) at the 29 m level in their measured outcrop section, showing that the stratigraphic interval described in that study can be assigned to sequences P1 and P2. Similarly, at Cerro Colorado the PE0.2 surface is correlative with the prominent intraformational unconformity interposed between a “lower allomember” and an “upper allomember” that, accordingly, are stratigraphically equivalent to sequences P1 and P2, respectively. This correlation is supported by biostratigraphic and radiometric dating (see below). The stratigraphic interval surrounding the P2-5 marker bed at Cerro la Bruja has been correlated with P2 strata of members D and E exposed at Cerro los Quesos (Fig. 5) that are bracketed between  $7.55 \pm 0.05$  Ma and  $6.93 \pm 0.09$  Ma (Di Celma et al. 2016a). Convincing correlation has been achieved by comparison of grain sizes, components, and both glass and mineral chemistry of some key ash layers. As a result, the P2-5 marker bed at Cerro la Bruja and the Condor marker bed at Cerro los Quesos are represented by volcanic ash

layers showing very similar features including color, convolute laminations, ash components, grain size, and dacitic volcanic glass composition. In the same sedimentary section, other ash beds show well assessed correspondence: CLQT23 at Cerro los Quesos and LB-T19 at Cerro la Bruja display the same grain size and components, and overlapping biotite and rhyolitic glass chemistry; CLQ-T21 at Cerro los Quesos and LB-T17 at Cerro la Bruja have similar glass chemistry.

The vertebrate content of this unit is known from various localities of the Ica Desert, including Cerro Colorado (“upper allomember” of Di Celma et al. 2016b; Bianucci et al. 2016c), Cerro los Quesos (members C-F of Di Celma et al. 2016b; Bianucci et al. 2016b), Cerro la Bruja (“La Bruja vertebrate level” of Muizon & DeVries 1985; Muizon 1988), Cerro Hueco la Zorra, Cerro Blanco, and Cerro Ballena. Some of the vertebrates detected in this unit are preserved within dolomite nodules, although this phenomenon is observed to a lesser extent than in the P1 sequence (Gariboldi et al. 2015). Mysticetes are represented by at least three medium- to large-sized species of balaenopterids including a form similar to extant *Megaptera* (humpback whale), and a diminutive cetotheriid (*Piscobalaena nana*). The toothed whales are well diversified. At least three different stem physeteroids are recognized thanks to a small number of specimens: *Acrophyseter robustus*, *Acrophyseter* sp., and an undescribed large-sized taxon (Muizon 1988; Lambert et al. 2014, 2017a). *Scaphokogia* and a new *Scaphokogia*-like kogiid (pygmy sperm whale) are also present in this unit with a few skulls. Ziphiids are uncommon but include at least four different species (all known from single specimens): the holotypes of *Chavinziphius maxillocristatus* and *Nazcacetus urbinai*, plus two other unnamed species based on more fragmentary remains (Lambert et al. 2009; Bianucci et al. 2016a, 2016b).

Delphinidans are relatively common, including the pontoporiid *Brachydelphis mazaesi* (also present in P1; known from the P2 sequence thanks to few specimens found near the PE0.2 unconformity), a phocoenid (cf. *Lomacetus ginsburgi*), and two kentriodontid-like delphinidans (*Atocetus iquensis* and *Belonodelphis peruanus*) (Muizon 1988). Pinnipeds are also present with at least one indeterminate species of monachine phocid (Muizon 1988; pers. obs.), whose remains (including some complete skeletons) are very common near the base of P2.

Among marine reptiles, a few specimens of a large undescribed chelonioid sea turtle and fragmentary remains referred to the gavialoid crocodylian aff. *Piscogavialis jugaliperforatus* have been detected. Birds are represented by a *Phalacrocorax*-like indeterminate cormorant; suliids and spheniscids (penguins) have also been reported (Muizon & DeVries 1985; Göhlich 2007; Stucchi 2007). Among the cartilaginous fish, *Carcharocles megalodon* and *Cosmopolitodus hastalis* are present besides a few other smaller sized species (including *Carcharhinus leucas* and *Myliobatis* sp.) (Muizon & DeVries 1985; Bianucci et al. 2016b; Landini et al. 2017). Remains of bony fish are also present in this unit; whereas most of them are still indeterminate, the presence of various well-preserved skulls of billfish (istiophorids and xiphiids) is remarkable (pers. obs.; Muizon & DeVries 1985). Cases of exceptional fossil preservation in the deposits referred to the P2 sequence include the phosphatized baleen of *Piscobalaena nana* (Marx et al. in press). The macro-invertebrate content of P2 is characterized by the disappearance of *Anadara sechurana* and *Miltha* sp. In the study area, at the base of this sequence, mollusks occur as dolomite internal molds of the bivalves *Dosinia ponderosa* and *Hybolophus* sp., and dolomite molds with gypsum-replaced shells of *Incatella hupei*. Above this base, at an unnamed cerro in the north-northwest of Cerros la Mama y la Hija (14°35'49"S - 75°41'33"W), a level yielded abundant specimens of *Hybolophus* sp. replaced by gypsum and, in some cases, filled by a dolomitized sediment, with well-preserved hinge and ornamentation; these remains probably belong to the species *H. maleficae* or *H. nelson* described by DeVries (2016). At Cerro los Quesos, a particular concentration of gypsum-replaced mollusks is present in the upper part of the stratigraphic succession (Member F of Di Celma et al. 2016b). The mollusks belong to the genus *Hybolophus* and regularly occur adjacent to the vertebrate fossils. At Cerro la Bruja few specimens of *Dosinia* sp. also occur as internal molds. Finally, at Cerro Blanco the P2 sequence shows the presence of barnacle plates and dolomite internal molds of mussels (Mytilidae), the latter never found in the previously described depositional sequences nor at other localities where the Pisco Formation crops out.

**Chronostratigraphic framework.** Integrated biostratigraphic analyses and radiometric ages

from airfall volcanic ashes provide the basis for a detailed chronostratigraphic framework for the portion of the Pisco Formation exposed in the study area and, in particular, to constrain the age of the three sequences described above.

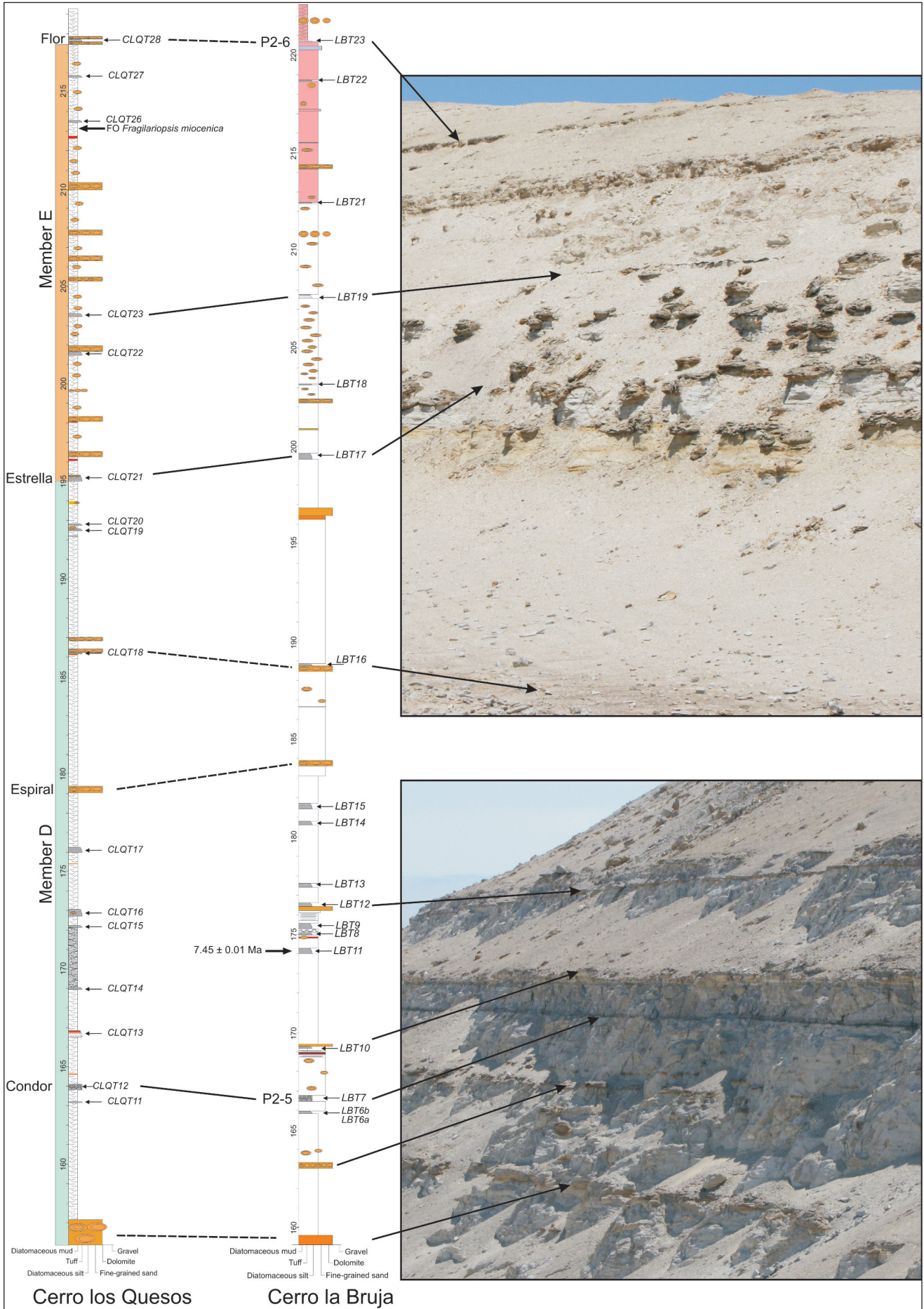
Diatom biostratigraphy of P1 and P2 has been described in depth at Cerro Colorado and Cerro los Quesos by Di Celma et al. (2016a, 2016b), Gariboldi (2016) and Gariboldi et al. (2017). The occurrences of diatom biostratigraphic markers at these two different sites were initially referred to the middle- to high-latitude zonation (Cerro Colorado, Di Celma et al. 2016b) and to the low-latitude diatom zonation (Cerro Los Quesos, Di Celma et al. 2016a) of Barron (1985) and bioevents were dated following the updated calibration of Barron (2003). Successively, Gariboldi et al. (2017) referred the biostratigraphy of both P1 and P2 to the low-latitude diatom zonation (Barron, 1985), using updated calibration of bioevents suggested by Barron (2003). Although both Gariboldi (2016) and Gariboldi et al. (2017) highlighted the need of a specific calibration of bioevents for the south tropical Pacific Ocean, biostratigraphic analyses are in general agreement with  $^{40}\text{Ar}/^{39}\text{Ar}$  ages.

#### *Chronostratigraphic framework for the P0 sequence.*

Due to the lack of biostratigraphic markers and datable ash layers, no direct information on the age of the P0 sequence is available so far. Its age, however, can be roughly constrained by those of the underlying Chilcatay Formation and the overlying P1.

An ash layer sampled in the fine-grained unit of the Chilcatay Formation, just 1 m below the PE0.0 erosional contact with the overlying P0 (14°35'40.2"S - 75°40'04.8"W), yielded an  $^{40}\text{Ar}/^{39}\text{Ar}$  age of  $17.99 \pm 0.10$  Ma. This age is also supported by recent data (Belia & Nick 2016) and biostratigraphic analyses. Indeed, although the lithology is mainly terrigenous, calcareous nannofossils and foraminifera are present at some carbonate-rich intervals. Foraminifera are recognizable in hand-samples but their tests are highly altered and cannot be extracted from the sediment. The nannofossil assemblages recovered from some of the samples are character-

Fig. 5 - Stratigraphic logs showing correlation of the sedimentary successions exposed at Cerro los Quesos and Cerro la Bruja. Solid and dashed connecting lines between sections represent certain and inferred correlations, respectively.



ized by long-ranging Oligocene-Miocene species with the youngest identified species represented by *Helicosphaera carteri*, documenting that the age is at least younger than 23 Ma. Abundant diatoms and silicoflagellates characterize the uppermost meters of this sediment succession. Among diatoms, the presence of *Cestodiscus pulchellus* and *Coscinodiscus lewisianus* constrains the age of these samples to older than 14 Ma, which is consistent with abundant *Distephanopsis crux* subsp. *parvus* and subsp. *scutulatus* and presence of *Corbisema triacantha* and *Stephanocha speculum* cf. *trionmata* among silicoflagellates.

#### *Chronostratigraphic framework for the P1 sequence.*

As reported by Gariboldi (2016) and Gariboldi et al. (2017), the P1 sequence is characterized by the co-occurrence of *Denticulopsis praekatayamae* and *Lithodesmium reynoldsii*. The interval characterized by these two species is well constrained between the First Occurrence of *D. praekatayamea* and the Last Occurrences of *L. reynoldsii*, calibrated at 9.5 Ma and 8.9 Ma, respectively (ages of appearance and extinction of middle-to-high-latitude planktonic diatoms in the North Pacific, Barron 2003). These diatom bioevents indicate the late Miocene *Thalassiosira yabei* zone (previously known as *Coscinodiscus yabei* zone) of the Pacific low Latitude zonation of Barron (1985). Other secondary marker species in P1 are rare specimens of *Koizumia tatsunokuchiensis* and unidentified plicated *Thalassiosira* specimens (Gariboldi 2016; Gariboldi et al. 2017). New  $^{40}\text{Ar}/^{39}\text{Ar}$  radiometric ages from volcanic ashes strongly support this interpretation and indicate an age of  $9.00 \pm 0.02$  Ma for the lower portion of this sequence at Cerros Cadenas de los Zanjones ( $14^{\circ}34'15.8''\text{S}$  -  $75^{\circ}43'44.2''\text{W}$ ) and  $9.10 \pm 0.04$  Ma for its middle part at Cerro Colorado.

#### *Chronostratigraphic framework for the P2 sequence.*

Diatom assemblages within P2 are characterized by rare specimens of diatom stratigraphic markers and specimens of *Thalassiosira* cf. *flexuosa* (Gariboldi 2016; Gariboldi et al. 2017). Marker species such as *Thalassiosira antiqua*, whose FO is calibrated by Barron (2003) at 8.5 Ma, *Fragilariopsis reinholdii*, *Koizumia tatsunokuchiensis* and *Nitzschia pliocena* characterize the assemblage but are not pivotal for age assignment. Only the interval of the P2 sequence embracing the P2-6 marker bed, characterized by the co-occurrence of *Fragilariopsis miocenica* and *Nitzschia*

*porteri*, can be constrained between 7.3 Ma and 7.1 Ma, which are the calibrated ages for the FO of *F. miocenica* and LO of *N. porteri*, respectively (Barron 2003; Gariboldi et al. 2017). These biostratigraphic age constraints agree with the radiometric age provided by an ash layer from this stratigraphic interval at Cerro la Bruja ( $14^{\circ}34'29''\text{S}$  -  $75^{\circ}39'53.7''\text{W}$ ), which yielded a consistent  $^{40}\text{Ar}/^{39}\text{Ar}$  age of  $7.45 \pm 0.01$  Ma (Fig. 5). This interval of the P2 sequence can therefore be assigned to the *Fragilariopsis miocenica* zone (previously known as *Nitzschia miocenica* zone) of the Pacific low Latitude zonation of Barron (1985), assessing a late Miocene age. Overall, the biostratigraphic age constraints discussed above are validated by  $^{40}\text{Ar}/^{39}\text{Ar}$  age determinations, which indicate that strata of the P2 sequence span, at least, the period between  $7.55 \pm 0.05$  Ma and  $6.71 \pm 0.02$  Ma (Di Celma et al. 2016a; Gariboldi et al. 2017).

## DISCUSSION

The recognition of three unconformity-bounded sediment units that can be correlated among different parts of the basin has been used to elucidate the sequence stratigraphic framework of the Pisco strata exposed in the study area. Viewed as a whole, the Pisco Formation comprises a wedge of sediment that thins to the northeast, a trend also apparent within each of the three component sequences (Fig. 6). These unconformity-bounded sediment packages, representing landward-stepping retrogradational events, onlap onto the underlying Chilcatay strata and basement rocks and progressively overstep them from southwest to northeast. Consequently, the basal contact of the Pisco Formation is an angular unconformity where it overlies older sediments of the Chilcatay Formation, or a nonconformity where it rests on crystalline basement rocks.

The excellent agreement between biostratigraphic data and a few well-constrained  $^{40}\text{Ar}/^{39}\text{Ar}$  radiometric ages from volcanic ash layers provides useful constraints on the depositional age of the three Pisco sequences exposed south of Cerro Blanco. At present, due to the lack of direct biostratigraphic and radiometric data, our best estimate of the age of P0 is between  $17.99 \pm 0.10$  Ma and  $9.00 \pm 0.02$  Ma, which are the available ages for the youngest sediments of the underlying Chilcatay Formation

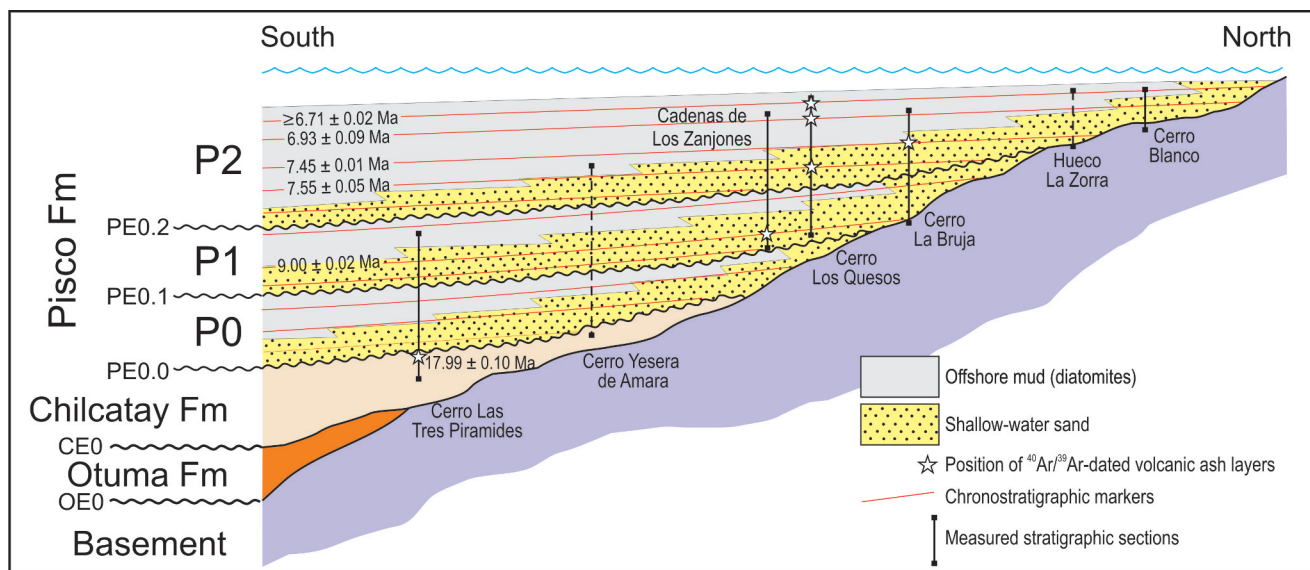


Fig. 6 - Schematic, dip-oriented stratigraphic diagram for the Pisco Formation (not in scale) showing the position of the stratigraphic sections on which the diagram is based (vertical black lines). These sections were supplemented by a cursory stratigraphic examination of two additional sites (vertical dashed lines). The Pisco Formation exhibits pronounced thinning to the northeast with component sequences onlapping onto the basal composite surface PE0 and arranged in a retrogradational pattern, progressively offset to the northeast. The marine erosion surfaces that bound Pisco sequences, namely PE0.0, PE0.1, and PE0.2, formed as a result of wave erosion in a transgressing shoreline following sea-level lowstand, and in consequence will be close to planar, and inclined slightly seaward. Red lines indicate chronostratigraphic markers (e.g., volcanic ash layers).

and for the onset of deposition of the overlying P1 strata, respectively. Diatom biostratigraphy and  $^{40}\text{Ar}/^{39}\text{Ar}$  radiometric ages converge to indicate that strata of the P1 sequence were deposited between about 9.5 Ma and 8.9 Ma, whereas those of the P2 sequence exposed in the study area are younger than 8.5 Ma and older than  $6.71 \pm 0.02$  Ma (Di Celma et al. 2016a; Gariboldi et al. 2017).

Our survey for fossil vertebrates outlines the outstanding paleontological value of the Pisco Formation, which stands out among Neogene marine deposits worldwide as a true Fossil-Lagerstätte. As reported above, the vertebrate content of P0 is still scarcely known; nevertheless, based on our preliminary investigations, it clearly differs from that of the overlying P1 sequence, especially with regard to the cetacean assemblage. The PE0.2 surface is characterized by a marked shift in composition and diversity of the vertebrate community. In P1, baleen-bearing whales are mainly represented by medium-sized cetotheriids, whereas larger balaenopterids are much less abundant; in contrast, in P2, balaenopterids dominate the mysticete assemblage, and cetotheriids are represented by a small number of specimens (assigned to *Piscobalaena nana*). With regard to the odontocetes, the PE0.2 surface records the disappearance of the stem beaked whale

species *Messapicetus gregarius* (one of the most common taxa in P1), replaced in P2 by other species of ziphiids (including *Chavinziphius maxillo cristatus* and *Nazcacetus urbina*); a turnover in the species of kentriodontid-like delphinidans is also observed. Stem physeteroids are present in both P1 and P2 with *Livyatan melvillei* only found in P1 and *Acrophyseter* spp. common in P2 and possibly already present in P1. The pontoporiid *Brachydelphis*, very common in P1, survives in the lower strata of the P2 sequence. Within P2, phocoenids and kogiids make their first appearance in the East Pisco basin. The P2 sequence also records the first occurrences of pinnipeds from the Pisco basin, represented by abundant specimens concentrated in the basal beds of this unit. Furthermore, disappearance of stem Sphenisciformes and first occurrences of crown penguins (Spheniscidae) are also documented in P2. The shark assemblage seemingly records a decline in diversity and disparity above the PE0.2 surface, with most selachian remains detected above this unconformity being referred to a few large species of Lamniformes.

In the Pisco Formation, the invertebrate biodiversity is rather low. *Dosinia* cf. *ponderosa* is the only molluscan species found in all of the three component sequences. An important faunal change has

been observed to occur through the PE0.1 unconformity, characterized by the appearance of a new fauna (*Anadara sechurana*, *Incatella hupei*, and species of *Hybolophus*, *Panopea* and *Trachicardium*), showing affinities with the middle Miocene Panamic fauna rather than with that of the lower to middle Miocene Navidad Formation of Chile (DeVries & Frassinetti 2003). The presence of *Anadara sechurana* in the upper part of the P1 sequence, above the ash layer dated at  $9.10 \pm 0.04$  Ma (Di Celma et al. 2016b), suggests that this species extends its range in the late Miocene. Both *A. sechurana* and *Miltha* sp. seem to disappear above the PE0.2 surface. The occurrence of mussels (Mytilidae), restricted at Cerro Blanco, is probably related to the presence of basement rocks providing hard substrates suitable for their proliferation. The identified bivalves associated with the vertebrate fossils in the Pisco Formation seem not to be typical of the Miocene whale-fall communities; according to Smith et al. (2015) these fossil communities are characterized by other genera, such as *Adipicola*, *Calyptogena*, *Conchocele*, *Idas*, *Solemya* and *Vesicomya*.

Detailed paleoecological investigations on the diatom assemblages still need to be developed. However, the necessity to shift from the middle- to high-latitude Pacific zonation of Barron (1985) to biostratigraphically date P1 (Di Celma et al. 2016b) to the low-latitude Pacific zonation of (Barron 1985) to date P2 (Di Celma et al. 2016a) is not accidental (Gariboldi et al. 2017). Indeed, diatom stratigraphic markers in P1 are those identified and used by Barron (1985) in the high-latitude Pacific zonation, while those in P2 are typical equatorial stratigraphic markers, suggesting that a regional ecological change characterizes the time period starting from the disappearance of *Thalassiosira antiqua* in P2.

## CONCLUSIONS

The stratigraphic architecture of the Pisco Formation, as delineated in this study, allows detailed correlations of chronostratigraphically significant stratal units among widely spaced outcrop sections. Due to recognition of three basin-wide unconformities (labelled PE0.0, PE0.1, and PE0.2 in ascending order), the Pisco strata exposed within the study area are interpreted to be composed of three depositional sequences, designated P0 through P2.

Bounding surfaces are transgressively modified sub-aerial unconformities that formed as a result of relative sea-level changes and mark abrupt basinward offsets in facies, so that shallower-water sand-rich deposits rest directly on deeper, diatomite-rich deposits. Internally, individual sequences exhibit similar facies progressions and display obvious lateral and vertical facies changes consisting of a retrogradational event in which downdip offshore diatomaceous mudstones step up over updip inner shelf and nearshore silty sandstones. Northeastward, successively younger sequences onlap progressively further onto the composite unconformity at the base of the Pisco Formation (PE0) and are organized in an overall retrogradational pattern.

Through integration of biostratigraphic and  $^{40}\text{Ar}/^{39}\text{Ar}$  radioisotopic age determinations, robust age constraints have been assigned to the three sequences identified in this study area. Based on the age of surrounding sediments, a conservative estimate of the age of P0 suggests deposition of these strata between  $17.99 \pm 0.10$  Ma and  $9.00 \pm 0.02$  Ma, whereas diatom biostratigraphy and calculated  $^{40}\text{Ar}/^{39}\text{Ar}$  ages converge to indicate that strata of the P1 sequence are younger than 9.5 Ma and older than 8.9 Ma and that those of the P2 sequence are younger than 8.5 Ma and older than  $6.71 \pm 0.02$  Ma. The vertebrate and macro-invertebrate assemblages of each of the three sequences recognized in the study area have been addressed. Our paleontological survey documents distinct shifts in the composition and diversity of these communities and provides a sound basis for general paleoecological reconstructions of the Upper Miocene faunas of the Pisco Formation.

*Acknowledgments.* This study was supported by grants from the Italian Ministry of University and Research to G. Bianucci (PRIN Project, 2012YJSBMK EAR-9317031), E. Malinverno (PRIN Project, 2012YJSBMK\_002), C. Di Celma (PRIN Project, 2012YJSBMK\_003), by the University of Pisa (PRA\_2015\_0028), and by a National Geographic Society Committee for Research Exploration grants (9410–13) to G. Bianucci. We thank W. Aguirre, A. Altamirano-Sierra, M.J. Laime, and B. Ramassamy for their help to prospect for fossil vertebrates during several fieldtrips in the investigated area. A particular thank to C. de Muizon, R. Salas-Gismondi, K. Post, and F. Marx for the useful discussions about the vertebrate fauna of the Pisco Formation and for their collaboration in the field and study of several fossils collected in the investigated area. The authors are especially grateful to T.J. DeVries for providing invaluable guidance to new field sites, help with identification of molluscan fossils, insightful discussions in the field, and comments on earlier versions of this work; responsibility for facts and interpretations nevertheless remains with the authors.

## REFERENCES

- Barron J.A. (1985) - Miocene to Holocene planktic diatoms. In: Bolli H.M., Saunders J.B. & Perch-Nielsen K.P. (Eds) - Plankton stratigraphy: 763-809. Cambridge Univ. Press, Cambridge.
- Barron J.A. (2003) - Planktonic marine diatom record of the past 18 my: appearances and extinctions in the Pacific and Southern Oceans. *Diatom Res.*, 18: 203-224.
- Belia E.R. & Nick K.E. (2016) - Early-Miocene calcareous nannofossil biostratigraphy from low-latitude, Pisco Basin, Peru. *Geol. Soc. Am. Abstracts with Programs*, 48: 4.
- Bianucci G., Di Celma C., Urbina M. & Lambert G. (2016a) - New beaked whales from the late Miocene of Peru and evidence for convergent evolution in stem and crown Ziphiidae (Cetacea, Odontoceti). *PeerJ* 4:e2479. DOI 10.7717/peerj.2479
- Bianucci G., Di Celma C., Collareta A., Landini W., Post K., Tinelli C., de Muizon C., Bosio G., Gariboldi K., Gioncada A., Malinverno E., Cantalamessa G., Altamirano-Sierra A., Salas-Gismondi R., Urbina M. & Lambert O. (2016b) - Fossil marine vertebrates of Cerro Los Quesos: Distribution of cetaceans, seals, crocodiles, seabirds, sharks, and bony fish in a late Miocene locality of the Pisco Basin, Peru. *J. Maps*, 12: 1037-1046.
- Bianucci G., Di Celma C., Landini W., Post K., Tinelli C., de Muizon C., Gariboldi K., Malinverno E., Cantalamessa G., Gioncada A., Collareta A., Salas-Gismondi R., Varas-Malca R.M., Urbina M. & Lambert O. (2016c) - Distribution of fossil marine vertebrates in Cerro Colorado, the type locality of the giant raptorial sperm whale *Livyatan melvillei* (Miocene, Pisco Formation, Peru). *J. Maps*, 12: 543-557.
- Bianucci G., Lambert O. & Post K. (2010) - High concentration of long-snouted beaked whales (genus *Messapicetus*) from the Miocene of Peru. *Palaeontology*, 53: 1077-1098.
- Boessenecker R.W., Perry F.A. & Schmitt J.G. (2014) - Comparative taphonomy, taphofacies, and bonebeds of the Mio-Pliocene Purisima Formation, Central California: strong physical control on marine vertebrate preservation in shallow marine settings. *PLoS ONE*, 9: e91419. doi:10.1371/journal.pone.0091419.
- Brand L.R., Esperante R., Chadwick A.V., Poma Porras O. & Alomía M. (2004) - Fossil whale preservation implies high diatom accumulation rate in the Miocene-Pliocene Pisco Formation of Peru. *Geology*, 32: 165-168.
- Brand L.R., Urbina M., Chadwick A., DeVries T.J. & Esperante R. (2011) - A high resolution stratigraphic framework for the remarkable fossil cetacean assemblage of the Miocene/Pliocene Pisco Formation, Peru. *J. South Am. Earth Sci.*, 31: 414-425.
- Chiocci F.L. & Clifton H.E. (1991) - Gravel-filled gutter casts in nearshore facies - indicators of ancient shoreline trend. In: From Shoreline to Abyss: Contributions in Marine Geology in Honor of Francis Parker Shepard. Osborne, R.H. (Ed.) - *SEPM Spec. Publ.*, 46: 67-76.
- Collareta A., Landini W., Chacaltana C., Valdivia W., Altamirano-Sierra A., Urbina M. & Bianucci G. (2017) - A well preserved skeleton of the fossil shark *Cosmopolitodus hastalis* from the late Miocene of Peru, featuring fish remains as fossilized stomach contents. *Riv. It. Paleontol. Strat.*, 123: 11-22.
- Collareta A., Landini W., Lambert O., Post K., Tinelli C., Di Celma C., Panetta D., Tripodi M., Salvadori P.A., Caramella D., Marchi D., Urbina M. & Bianucci G. (2015) - Piscivory in a Miocene Cetotheriidae: first record of fossilized stomach content for an extinct baleen-bearing whale. *Sci. Nature*, 102: article no. 70.
- DeVries T.J. (1998) - Oligocene deposition and Cenozoic sequence boundaries in the Pisco Basin (Peru). *J. South Am. Earth Sci.*, 11: 217-231.
- DeVries T.J. (2006) - A new early Miocene *Muracypraea* Woodring, 1957 (Gastropoda: Cypraeidae) from the Pisco Basin of southern Peru. *The Nautilus*, 120: 101-105.
- DeVries T.J. (2007) - Cenozoic Turritellidae (Gastropoda) from Southern Peru. *J. Paleontol.*, 81: 331-351.
- DeVries T.J. (2016) - Fossil Cenozoic crassatelline bivalves from Peru: New species and generic insights. *Acta Palaeontol. Pol.*, 61: 661-688.
- DeVries T.J. & Frassinetti D. (2003) - Range extensions and biogeographic implications of Chilean Neogene mollusks found in Peru. *Bol. Mus. Nacion. Hist. Nat., Chile*, 52: 119-135.
- DeVries T.J. & Schrader H. (1997) - Middle Miocene marine sediments in the Pisco Basin (Peru). *Bol. Soc. Geol. Perú*, 87: 1-13.
- Di Celma C., Malinverno E., Cantalamessa G., Gioncada A., Bosio G., Villa I.M., Gariboldi K., Rustichelli A., Pierantoni P.P., Landini W., Tinelli C., Collareta A. & Bianucci G. (2016a) - Stratigraphic framework of the late Miocene Pisco Formation at Cerro Los Quesos (Ica Desert, Peru). *J. Maps*, 12: 1020-1028.
- Di Celma C., Malinverno E., Gariboldi K., Gioncada A., Rustichelli A., Pierantoni P.P., Landini W., Bosio G., Tinelli C. & Bianucci G. (2016b) - Stratigraphic framework of the late Miocene to Pliocene Pisco Formation at Cerro Colorado (Ica Desert, Peru). *J. Maps*, 12: 515-557.
- Dunbar R.B., Marty R.C. & Baker P.A. (1990) - Cenozoic marine sedimentation in the Sechura and Pisco basins, Peru. *Palaeogeogr., Palaeoclimatol., Palaeoecol.*, 77: 235-261.
- Esperante R., Brand L.R., Chadwick A.V. & Poma O. (2015) - Taphonomy and paleoenvironmental conditions of deposition of fossil whales in the diatomaceous sediments of the Miocene/Pliocene Pisco Formation, southern Peru - a new fossil-lagerstätte. *Palaeogeogr., Palaeoclimatol., Palaeoecol.*, 417: 337-370.
- Esperante R., Brand L.R., Nick K.E., Poma O. & Urbina M. (2008) - Exceptional occurrence of fossil baleen in shallow marine sediments of the Neogene Pisco Formation, Southern Peru. *Palaeogeogr., Palaeoclimatol., Palaeoecol.*, 257: 344-360.
- Föllmi K.B. (2016) - Sedimentary condensation. *Earth-Sci. Rev.*, 152: 143-180.
- Gariboldi K. (2016) - A note on diatom stratigraphic markers in upper Miocene sediments of the Pisco Formation,

- Peru, and description of *Delphineis urbinai* sp. nov. *Diatom Res.*, 31: 285-301.
- Gariboldi K., Bosio G., Malinverno E., Gioncada A., Di Celma C., Villa I.M., Urbina M. & Bianucci G. (2017) - Biostratigraphy, geochronology and sedimentation rates of the upper Miocene Pisco Formation at two important marine vertebrate fossil-bearing sites of southern Peru. *Newsl. Stratigr.*, 50: DOI: 10.1127/nos/2017/0345.
- Gariboldi K., Gioncada A., Bosio G., Malinverno E., Di Celma C., Tinelli C., Cantalamessa G., Landini W., Urbina M. & Bianucci G. (2015) - The dolomitic nodules enclosing fossil marine vertebrates in the East Pisco Basin, Peru: field and petrographic insights into their genesis and role in preservation. *Palaeogeogr., Palaeoclimatol., Palaeoecol.*, 438: 81-95.
- Gioncada A., Collareta A., Gariboldi K., Lambert O., Di Celma C., Bonaccorsi E., Urbina M. & Bianucci G. (2016) - Inside baleen: Exceptional microstructure preservation in a late Miocene whale skeleton from Peru. *Geology*, 44: 839-842.
- Göhlich U.B. (2007) - The oldest fossil record of the extant penguin genus *Spheniscus*-a new species from the Miocene of Peru. *Acta Palaeontol. Pol.*, 52: 285-298.
- Grimm K.A. (2000) - Stratigraphic condensation and the reposition of economic phosphorite: Allostratigraphy of Oligo-Miocene shelfal sediments, Baja California Sur, Mexico. In C.R. Glenn, L. Prévôt-Lucas and J. Lucas (Eds), *Marine Authigenesis: From Microbial to Global, SEPM Spec. Publ.*, 66: 325-347.
- Hampel A. (2002) - The migration history of the Nazca Ridge along the Peruvian active margin: a re-evaluation. *Earth Planet. Sci. Letters*, 203: 665-679.
- Hsu J.T. (1992) - Quaternary uplift of the Peruvian coast related to the subduction of the Nazca Ridge: 13.5 to 15.6 degrees south latitude. *Quatern. Intern.*, 15/16: 87-97.
- Kidwell S.M. (1989) - Stratigraphic condensation of marine transgressive records: origin of major shell deposits in the Miocene of Maryland. *J. Geol.*, 97: 1-24.
- Lambert O., Bianucci G. & Beatty B.L. (2014) - Bony outgrowths on the jaws of an extinct sperm whale support macroraptorial feeding in several stem physeteroids. *Naturwissenschaften*, 101: 517-521.
- Lambert O., Bianucci G. & Post K. (2009) - A new beaked whale (Odontoceti, Ziphiidae) from the Middle Miocene of Peru. *J. Vert. Paleontol.*, 29: 910-922.
- Lambert O., Bianucci G. & Post K. (2010a) - Tusk bearing beaked whales from the Miocene of Peru: Sexual dimorphism in fossil ziphiids? *J. Mammal.*, 91: 19-26.
- Lambert O., Bianucci G. & Muizon C. de. (2017a) - Macroraptorial sperm whales (Cetacea, Odontoceti, Physeteroidea) from the Miocene of Peru. *Zool. J. Linn. Soc.*, 179: 404-474.
- Lambert O., Bianucci G., Post K., Muizon C. de, Salas-Gismondi R., Urbina M. & Reumer J. (2010b) - The giant bite of a new raptorial sperm whale from the Miocene epoch of Peru. *Nature*, 466: 105-108.
- Lambert O., Bianucci G., Urbina M. & Geisler J.H. (2017b) - A new iniod (Cetacea, Odontoceti, Delphinidae) from the Miocene of Peru and the origin of modern dolphin and porpoise families. *Zool. J. Linn. Soc.* 179(4): 919-946.
- Lambert O., Collareta A., Landini W., Post K., Ramassamy B., Di Celma C., Urbina M. & Bianucci G. (2015) - No deep diving: evidence of predation on epipelagic fish for a stem beaked whale from the late Miocene of Peru. *Proc. Royal Soc. London Part B: Biol. Sci.*, 282: article no. 20151530.
- Landini W., Altamirano-Sierra A., Collareta A., Di Celma C., Urbina M. & Bianucci G. (2017) - The late Miocene elasmobranch assemblage from Cerro Colorado (Pisco Formation, Peru). *J. South Am. Earth Sciences*, 73: 168-190.
- Leckie D.A. & Walker R.G. (1982) - Storm- and tide-dominated shorelines in Cretaceous Moosebar-Lower Gates interval: Outcrop equivalents of Deep Basin gas trap in western Canada. *Am. Ass. Petrol. Geol. Bull.*, 66: 138-157.
- León W., Aleman A., Torres V., Rosell W. & De La Cruz O. (2008) - Estratigrafía, sedimentología y evolución tectónica de la cuenca Pisco Oriental. *Boletín INGEMMET*, 27 (Serie D), 144 pp.
- Macharé J., DeVries T., Barron J. & Fourtanier E. (1988) - Oligo-Miocene transgression along the Pacific margin of South America: New paleontological and geological evidence from the Pisco Basin, Peru. *Geodynamique*, 3: 25-37.
- Macharé J. & Ortlieb L. (1992). Plio-Quaternary vertical motions and the subduction of the Nazca Ridge, central coast of Peru. *Tectonophysics*, 205: 97-108.
- Marx F., Collareta A., Gioncada A., Post K., Lambert O., Bonaccorsi E., Urbina M. & Bianucci G. (in press) - How whales used to filter: exceptionally preserved baleen in a Miocene cetotheriid. *J. Anat.*, DOI:10.1111/joa.12622.
- Massari F. & Chiocci F. (2006) - Biocalcarene and mixed cool-water prograding bodies of the Mediterranean Pliocene and Pleistocene: architecture, depositional setting and forcing factors. In: Pedley H.M. & Carannante G. (Eds) - *Cool-Water Carbonates: Depositional Systems and Palaeoenvironmental Controls. Geol. Soci., London, Spec. Publ.*, 255: 95-120.
- Muizon C. de & DeVries T.J. (1985) - Geology and paleontology of late Cenozoic marine deposits in the Sacaco area (Peru). *Geol. Rund.* 74: 547-563.
- Muizon C. de. (1988) - Les vertébrés fossiles de la Formation Pisco (Pérou). Troisième partie: Les Odontocètes (Cetacea, Mammalia) du Miocène. *Trav. Inst. Français Et. Andines*, 42: 1-244.
- Mukasa S.B. & Henry D.J. (1990) - The San Nicolás Batholith: evidence for an early Palaeozoic magmatic arc along the continental or continental rift magmatism? *J. Geol. Soc., London*, 147: 27-39.
- Myrow P.M. (1992) - Pot and gutter casts from the Chapel Island Formation, southeast Newfoundland. *J. Sed. Petrol.*, 62: 992-1007.
- Parham J.F. & Pyenson N.D. (2010) - New sea turtle from the Miocene of Peru and the iterative evolution of feeding ecomorphologies since the Cretaceous. *J. Paleontol.*, 84: 231-247.
- Pemberton S.G. & MacEachern J.A. (1995) - The sequence

- stratigraphic significance of trace fossils: examples from the Cretaceous foreland basin of Alberta, Canada. In: J.C. Van Wagoner & G. Bertram (Eds) - Sequence stratigraphy of foreland basin deposits-outcrop and subsurface examples from the Cretaceous of North America. *AAPG Memoir*, 64: 429-475.
- Pomar L. & Tropeano M. (2001) - The Calcarene di Gravina Formation in Matera (Southern Italy): new insights for coarse-grained, large-scale, crossbedded bodies encased in offshore deposits. *AAPG Bull.*, 85: 661-689.
- Smith C.R., Glover A.G., Treude T., Higgs N.D. & Amon D.J. (2015) - Whale-fall ecosystems: recent insights into ecology, paleoecology, and evolution. *Ann. Rev. Mar. Sci.*, 7: 571-596.
- Stucchi M. (2007) - Los pingüinos de la Formación Pisco (Neógeno), Perú. In: Díaz-Martínez E., Rábano I. (Eds) - 4th European Meeting on the Palaeontology and Stratigraphy of Latin America, Madrid, España. *Cuad. Mus. Geom.*, 8: 367-373.
- Stucchi M., Varas-Malca R.M. & Urbina-Schmitt M. (2016) - New Miocene sulid birds from Peru and considerations on their Neogene fossil record in the Eastern Pacific Ocean. *Acta Palaeontol. Pol.*, 61: 417-427.
- Thornburg T.M. & Kulm L.D. (1981) - Sedimentary basins of the Peru continental margin: Structure, stratigraphy, and Cenozoic tectonics from 6°S to 16°S latitude. In: Kulm L.D., Dymond J., Dasch E.J. & Hussong D.M. (Eds) - Nazca plate: Crustal formation and Andean convergence. *Geol. Soc. America, Mem.*, 154: 393-422.
- Villa I.M., Hermann J., Müntener O. & Trommsdorff V. (2000) - <sup>39</sup>Ar / <sup>40</sup>Ar dating of multiply zoned amphibole generations (Malenco, Italian Alps). *Contrib. Miner. Petrol.*, 140: 363-381.
- von Huene R., Pecher I.A. & Gutscher M.-A. (1966) - Development of the accretionary prism along Peru and material flux after subduction of Nazca Ridge. *Tectonics*, 15: 19-33.
- Zúñiga-Rivero F. J., Klein G.D., Hay-Roe H. & Álvarez-Calderon E. (2010) - The hydrocarbon potential of Peru. BPZ Exploración & Producción S.R.L., Lima, Peru, 338 pp.

**APPENDIX 1**

The invertebrate taxa mentioned in the text, in systematic order. The suprageneric taxa follow WoRMS (accessed on Jan. 24, 2017). Specimens belonging to the taxa marked with \* have been collected during the present research.

**PHYLUM: MOLLUSCA****Class: BIVALVIA**

- SUPERFAMILY: Arcoidea \*  
 Family: Arcidae Lamarck, 1809 \*  
 Genus: *Anadara* Gray, 1847 \*  
*Anadara sechurana* Olsson, 1932 \*
- SUPERFAMILY: Cardioidea \*  
 Family: Cardiidae Lamarck, 1809 \*  
 Genus: *Trachycardium* Mörch, 1853 \*
- SUPERFAMILY: Crassatelloidea \*  
 Family: Crassatellidae Férussac, 1822 \*  
 Genus: *Hybolophus* Stewart, 1930 \*  
*Hybolophus maleficus* DeVries, 2016  
*Hybolophus nelsoni* (Grzybowski, 1899)
- SUPERFAMILY: Hiatelloidea \*  
 Family: Hiatellidae Gray, 1824 \*  
 Genus: *Panopea* Ménard de la Groye, 1807 \*
- SUPERFAMILY: Lucinoidea \*  
 Family: Lucinidae Fleming, 1828 \*  
 Genus: *Miltha* H. Adams et A. Adams, 1857 \*
- Family: Thyasiridae Dall, 1901  
 Genus: *Conchocele* Gabb, 1866
- SUPERFAMILY: Mytiloidea \*  
 Family: Mytilidae Rafinesque, 1815 \*  
 Genera: *Adipicola* Dautzenberg, 1927  
*Idas* Jeffreys, 1876
- SUPERFAMILY: Ostreoida \*  
 Family: Ostreidae Rafinesque, 1815 \*
- SUPERFAMILY: Solemyoidea  
 Family: Solemyidae Gray, 1840  
 Genus: *Solemya* Lamarck, 1818
- SUPERFAMILY: Veneroidea \*  
 Family: Veneridae Rafinesque, 1815 \*  
 Genera: *Amiantis* Carpenter, 1864  
*Chionopsis* Olsson, 1932 \*  
*Dosinia* Scopoli, 1777 \*  
*Dosinia ponderosa* (Gray, 1838) \*
- SUPERFAMILY: undefined  
 Family: Vesicomomyidae Dall et Simpson, 1901  
 Genera: *Calyptogena* Dall, 1891  
*Vesicomya* Dall, 1886

**Class: GASTROPODA**

- SUPERFAMILY: Architectonicoidea \*  
 Family: Architectonicidae Gray, 1850 \*
- SUPERFAMILY: Cerithioidea \*  
 Family: Turritellidae Lovén, 1847 \*  
 Genera: *Turritella* Lamarck, 1799 \*  
*Turritella infracarinata* Grzybowski, 1899  
*Incatella* (DeVries, 2007) \*  
*Incatella hupei* Nielsen in DeVries 2007 \*
- SUPERFAMILY: Cypraeoidea \*  
 Family: Cypraeidae Rafinesque, 1815 \*  
 Genus: *Muracypraea* Woodring, 1957  
*Muracypraea ormenoi* DeVries, 2006

- SUPERFAMILY: Ficoidea  
 Family: *Ficidae* Meek, 1864  
 Genus: *Ficus* Röding, 1798  
*Ficus distans* Sowerby, 1846
- SUPERFAMILY: Muricoidea  
 Family: Muricidae Rafinesque, 1815  
 Genus: *Tactilispina* DeVries, 2005  
*Tactilispina vermeiji* DeVries, 2005
- SUPERFAMILY: Tonnoidea \*

**PHYLUM: OCHROPHYTA****Class: BACILLARIOPHYCEAE (DIATOMS)**

- Genus: *Cestodiscus* Greville, 1865 \*  
*Cestodiscus pulchellus* Greville, 1866 \*
- Genus: *Coscinodiscus* Ehrenberg, 1839 \*  
*Coscinodiscus lewisianus* Greville, 1866 \*
- Genus: *Denticulopsis* Simonsen, 1979 \*  
*Denticulopsis praekatayamae* Yanagisawa et Akiba, 1990 \*
- Genus: *Fragilariopsis* Hustedt in Schmidt et al., 1913 \*  
*Fragilariopsis reinboldii* (Kanaya et Koizumi) Zielinski et Gersonde, 2002\*  
*Fragilariopsis miocenica* (Burckle) Censarek et Gersonde, 2002 \*
- Genus: *Koizumia* Yanagisawa, 1994 \*  
*Koizumia tatsunokuchiensis* (Koizumi) Yanagisawa, 1994 \*
- Genus: *Lithodesmium* Ehrenberg, 1839 \*  
*Lithodesmium reynoldsii* Barron, 1976 \*
- Genus: *Nitzschia* Hassall, 1845 \*  
*Nitzschia pliocena* (Brun) Mertz, 1966 \*  
*Nitzschia porteri* Frenguelli sensu Burckle, 1972 \*
- Genus: *Thalassiosira* Cleve, 1873 \*  
*Thalassiosira antiqua* (Grunow) Cleve-Euler, 1941 \*  
*Thalassiosira flexuosa* (Brun, 1894) Akiba and Yanagisawa, 1986  
*Thalassiosira yabei* (Kanaya 1959) Akiba and Yanagisawa, 1986

**Class: DICTYOCOPHYCEAE (SILICOFLAGELLATES)**

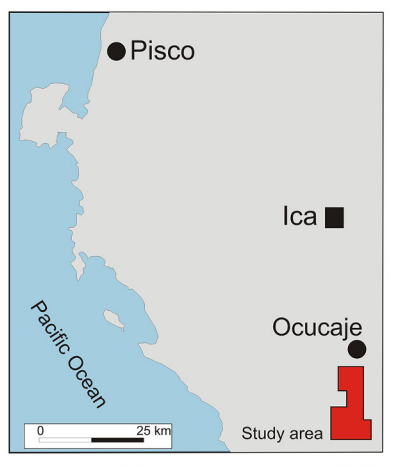
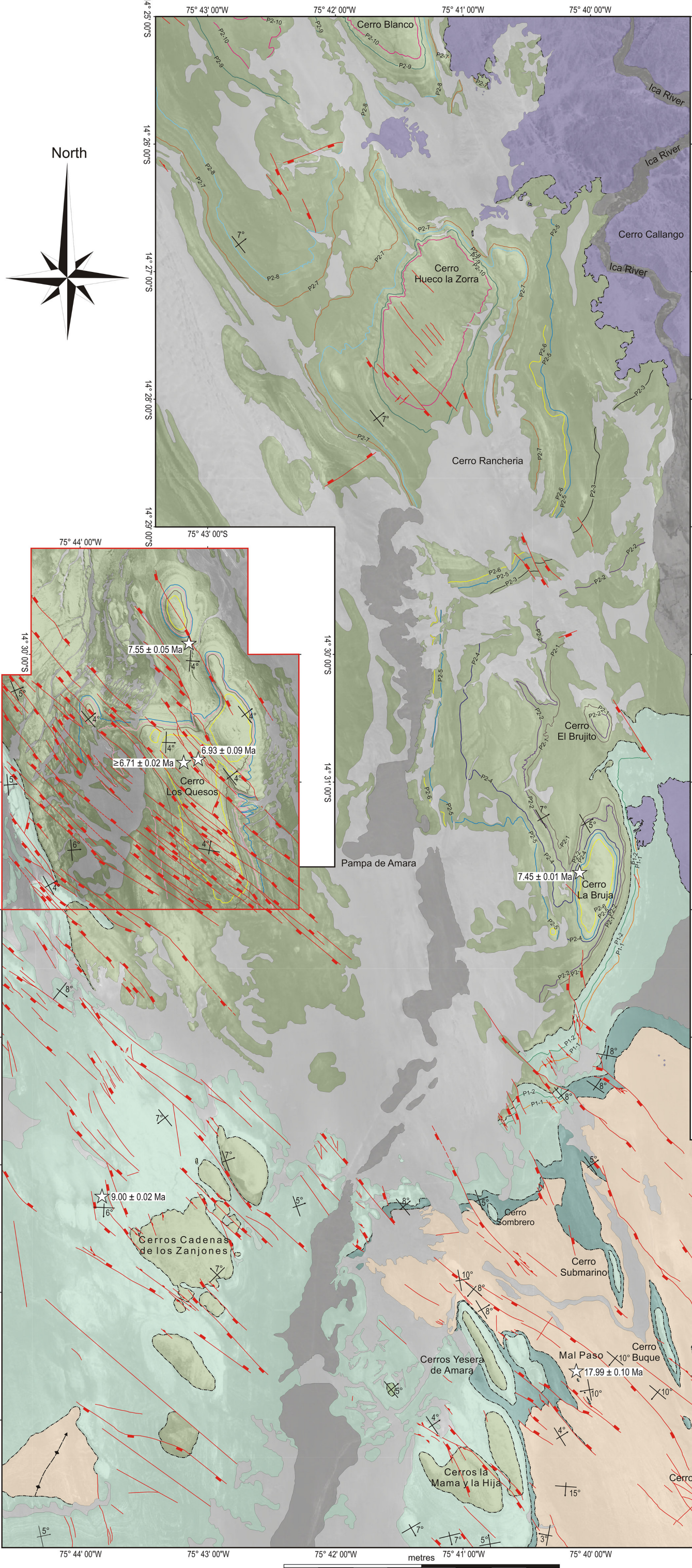
- Genus: *Corbisema* Hanna, 1928 \*  
*Corbisema triacantha* (Ehrenberg, 1844) Hanna, 1931 \*
- Genus: *Distephanopsis* Dumitrica, 1978 \*  
*Distephanopsis crux* subsp. *parva* (Bachmann, 1967) Desikachary et Prema, 1996 \*  
*Distephanopsis crux* subsp. *scutulata* (Bukry, 1982) Desikachary et Prema, 1996 \*
- Genus: *Stephanocha* McCartney et Jordan, 2015\*  
*Stephanocha speculum* var. *trionmata* (Ehrenberg, 1839) McCartney et Jordan, 2015

**PHYLUM: HAPTOPHYTA****Class: PRYMNESIOPHYCEAE (COCCOLITHOPHORES)**

- Helicosphaera carteri* (Wallich, 1877) Kamptner, 1954 \*

## **APPENDIX 2**

Fig. 2 - Location maps and geology of the western side of the Ica River valley. The geological map of the Cerro los Quesos area (red frame in the central western part) has been modified from Di Celma et al. (2016a). The Google Earth image shows the present study area (white frame) and location of the four stratigraphic sections measured at Cerro las Tres Piramides (CTP), Cadenas de los Zanjones (CZ), Cerro La Bruja (CLB), and Cerro Blanco (CB). The areas in the black frame (Cerro Colorado, CC) and in the red frame (Cerro los Quesos, CLQ) have been mapped by Di Celma et al. (2016b) and Di Celma et al. (2016a), respectively.



## LEGEND

- Quaternary surficial map units**
- Eolian sands and colluvium (Holocene and upper Pleistocene)
  - Alluvial gravels (Holocene and Pleistocene)
- Cenozoic units**
- Pisco Formation (late Miocene)**
- P2-10
  - P2-9
  - P2-8
  - P2-7
  - P2-6
  - P2-5
  - P2-4
  - P2-3
  - P2-2
  - P2-1
- Cerro la Bruja - Cerro Blanco**
- P1-2
  - P1-1
- Cerro los Quesos**
- Flor
  - Estrella
  - Espiral
  - Cóndor
- P0 Sequence**
- PE0.2 unconformity
  - PE0.1 unconformity
  - PE0.0 unconformity
- Chilcatay Formation (late Oligocene-early middle Miocene)**
- Massive, medium- to fine-grained sandstones and siltstones (>70 m thick) underlying and laterally interfingering with a coarse-grained, SW-dipping, basinward-prograding heterozoan carbonate wedge (10 to 35 m thick). The clinostriated calcarenitic wedge is unconformably overlain by a fining-upward facies succession composed of basal sandstones gradually overlain by massive siltstones (10 to 25 m-thick).
- Basement (pre-Cenozoic)**
- Lower Paleozoic gabbroic to granitoid rocks (San Nicolas batholith) and Jurassic volcano-sedimentary rocks (Guaneros Formation)
- PE0 unconformity**
- Unconformity-bounded depositional sequences (P0, P1 and P2) of shelf origin displaying an overall fining-upward trend. Vertical progression of facies within each sequence includes nearshore conglomerates and thoroughly bioturbated, fine-grained sandstones grading upwards into offshore sandy siltstones and/or diatomaceous mudstones with minor additions of sandstones, dolomitic horizons, and ash layers. The formation contains a rich and well-preserved vertebrate fauna.

- Symbols**
- ☆ <sup>40</sup>Ar/<sup>39</sup>Ar radioisotopic age
  - 9° Strike and dip of bedding
  - Normal faults. Rectangles on downthrown block
  - Plunging anticline, axial trace

